1B5-2

Comparison of Crosstalk Analysis Methods for Shifted Parallel-Coupled Lines on a PCB

#Jae Kwon Han [1], Jae Cheol Ju [2], and Dong Chul Park [1]
[1] Department of Radio Science and Engineering, Chungnam National University
220 Gung-dong, Yuseong-gu, Daejeon, Korea (jamtan@cnu.ac.kr)
[2] Samsung Electro-Mechanics Co., Ltd.

1. Introduction

As the circuit density of pattern traces and the data rate on a printed circuit board (PCB) is increased, an unexpected electromagnetic interference (EMI) such as crosstalk can degrade the intended signal transmission.

The crosstalk problems on multiconductor transmission lines (MTLs) which are parallel and have the same length have been researched by C. R. Paul[1]. In case of shifted parallel-coupled lines as shown in Fig. 1, the crosstalk can be analyzed by using 1-D FDTD (Finite-Difference Time-Domain) method based on the MTL equations[2]. The shifted parallel-coupled lines are divided into three regions, which are uncoupled line section in line #1, parallel-coupled line section in line #1 and #2, and uncoupled line section in line #2. The uncoupled line section is represented by self-capacitance and self-inductance and the coupled line section is represented by self- and mutual-capacitance and inductance matrices. On the other hand, Kami[3] suggested a circuit-concept approach by which the crosstalk analysis between two transmission lines of finite length in arbitrary directions is analytically possible. His approach can also be applied to the case of the shifted parallel-coupled lines.

In this paper, the crosstalk phenomena of shifted parallel-coupled lines on a PCB are investigated using 1-D FDTD method and the circuit-concept approach, respectively. Also, the theoretical results of these two approaches are compared with the HFSS simulation and the measurement.

2. 1-D FDTD Equations

The MTL equations for lossless case are given in matrix form as follows[1],[2]:

$$\frac{\partial[V(z,t)]}{\partial z}+[L]\frac{\partial[I(z,t)]}{\partial t}=0, \qquad \frac{\partial[I(z,t)]}{\partial z}+[C]\frac{\partial[V(z,t)]}{\partial t}=0 \tag{1}$$

where $[V(z,t)]$ and $[I(z,t)]$ are a line voltage matrix and a line current matrix along the line in longitudinal axis, z, respectively. $[L]$ and $[C]$ are per-unit-length inductance matrix and capacitance matrix, respectively. The line parameters $[L]$ and $[C]$ can be determined from cross-sectional information of given line.

The terminal conditions represented as generalized Thevenin equivalents are

$$[V(0,t)]=[V_s(t)]-[R_s][I(0,t)], \qquad [V(l,t)]=[V_l(t)]-[R_l][I(l,t)] \tag{2}$$

where $[V_s(t)]$ and $[V_l(t)]$ are independent source voltages at z=0 and z=l, respectively. $[R_s]$ and $[R_l]$ are lumped source and load resistances, respectively.

The FDTD method is a common way to solve the MTL equations. Fig. 1 shows the FDTD grid for the shifted parallel-coupled lines on a PCB. Sections 1 and 3 consist of uncoupled transmission line #1 and #2. Therefore, only the self-capacitance and the self-inductance are needed to calculate the line voltage and current at each node. Firstly, the FDTD equations expressed by (3)

ISBN: 978-4-88552-223-9 C3055©IEICE

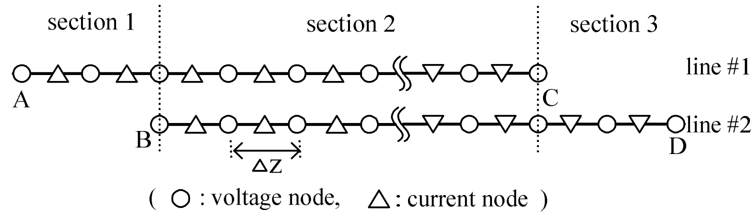

Figure 1: The FDTD grid of shifted-parallel coupled lines on a PCB

and (4) can be obtained by incorporating the terminal conditions with (2) at nodes A and C in line #1 and B and D in line #2 in Fig. 1. In (4), *NDZ* is the number of the length Δz. Secondly, the voltage and the current at each node in section 1 and 3 except the terminal nodes can be obtained by using (5) and (6). Finally, the voltage and the current at each node in section 2 can be similarly obtained by using (5) and (6). In this case C and L denote $[C]_{2\times2}$ and $[L]_{2\times2}$ matrices, respectively.

$$V_1^{n+1} = \left(\frac{\Delta z}{\Delta t} R_s C + 1\right)^{-1} \times \left[\left(\frac{\Delta z}{\Delta t} R_s C - 1\right) V_1 - 2R_s I_1^{n+1/2} + \left(V_s^{n+1} + V_s^{n}\right)\right] \tag{3}$$

$$V_{NDZ+1}^{n+1} = \left(\frac{\Delta z}{\Delta t} R_L C + 1\right)^{-1} \times \left[\left(\frac{\Delta z}{\Delta t} R_L C - 1\right) V_{NDZ+1}^{n} - 2R_L I_{NDZ}^{n+1/2} + \left(V_L^{n+1} + V_L^{n}\right)\right] \tag{4}$$

$$V_k^{n+1} = V_k^{n} - \frac{\Delta t}{\Delta z} C^{-1}\left(I_k^{n+1/2} - I_{k-1}^{n+1/2}\right), \qquad k=2,\bullet\bullet\bullet, NDZ \tag{5}$$

$$I_k^{n+3/2} = I_k^{n+1/2} - \frac{\Delta t}{\Delta z} L^{-1}\left(V_{k+1}^{n+1} - V_{k-1}^{n-1}\right), \qquad k=1,\bullet\bullet\bullet, NDZ \tag{6}$$

3. Circuit-Concept Approach

Fig. 2 shows the structure of two coupled lines of finite length in arbitrary directions above a ground plane. It is set that l_1, h_1 and l_2, h_2 are the length of the line and the thickness of substrate, respectively. θ is the angle between the axes x_1 and x_2. If each cross-section of transmission lines is very small compared to wavelength, the propagation mode of two transmission lines will be TEM.

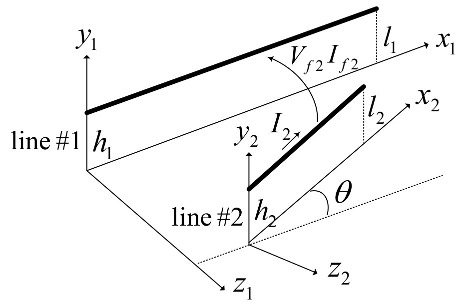

Figure 2: Non-parallel coupled microstrip lines

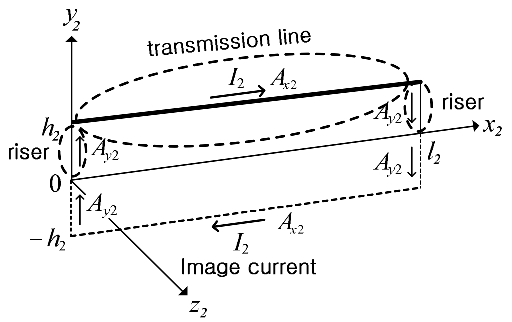

Figure 3: Image current and vector magnetic potential of a microstrip line

In calculating the crosstalk between coupled microstrip lines one line driven by a lumped source acts as a transmitting antenna. This line can be referred to as a generator line and affects the neighboring line. The neighboring line which is nearly located in a generator line plays the role of a receiving antenna and can be referred to as a receptor line. For example, if we consider line #2 as a generator line in Fig. 2, the line #1 is exposed to external electromagnetic field due to the current flowing on line #2. Therefore, the modified telegrapher equations and its solution for the line voltage $V_1(x)$ and current $I_1(x)$ on line #1 can be expressed as[3]:

$$-\frac{d}{dx}\begin{bmatrix} V_1(x_1') \\ I_1(x_1') \end{bmatrix} = \begin{bmatrix} 0 & j\omega L_1 \\ j\omega C_1 & 0 \end{bmatrix}\begin{bmatrix} V_1(x_1') \\ I_1(x_1') \end{bmatrix} + \begin{bmatrix} V_{f2}(x_1') \\ I_{f2}(x_1') \end{bmatrix} \tag{7}$$

$$\begin{bmatrix} V_1(0) \\ I_1(0) \end{bmatrix} = F_1(l_1)\begin{bmatrix} V_1(l_1) \\ I_1(l_1) \end{bmatrix} - \int_0^{l_1} F_1(x_1')\begin{bmatrix} V_{f2}(x_1') \\ I_{f2}(x_1') \end{bmatrix} \tag{8}$$

where C_1 and L_1 are the per-unit-length self-capacitance and self-inductance of line #1, respectively, ω is the angular frequency, and F_1 is a chain matrix. In (7) and (8), $V_{f2}(x_1)$ and $I_{f2}(x_1)$, the forcing terms, denote the line voltage and current on line #1 due to the magnetic and electric coupling caused by current I_2 that flows the transmission line section and riser section of line #2 as shown in Fig. 3 and can be expressed using the vector magnetic potential as:

$$\begin{bmatrix} V_{f2}(x_1') \\ I_{f2}(x_1') \end{bmatrix} = \begin{bmatrix} -j\omega\int_0^{h_1}\left(\frac{\partial A_{y1}}{\partial x_1} - \frac{\partial A_{x1}}{\partial y_1}\right)dy_1' \\ j\omega C_1\left\{\int_0^{h_1} - j\omega A_{y1}dy_1' + \frac{(\nabla\cdot\vec{A}_1)\big|_0^{h_1}}{j\omega\mu_0\varepsilon_0}\right\} \end{bmatrix} \tag{9}$$

The x-component and the y-component of the vector magnetic potential generated by current I_2 flowing on line #2 and through the risers as shown in Fig. 3 are expressed as:

$$A_{x2} = \frac{\mu_0}{4\pi}\left\{\int_0^{l_2} I_2(x_2')\frac{\exp(-j\beta R_{x1})}{R_{x1}}dx_2' - \int_0^{l_2} I_2(x_2')\frac{\exp(-j\beta R_{x2})}{R_{x2}}dx_2'\right\} \tag{10}$$

$$A_{y2} = \frac{\mu_0}{4\pi}\left\{\int_{-h_2}^{h_2} I_2(0)\frac{\exp(-j\beta R_{y1})}{R_{y1}}dy_2' - \int_{-h_2}^{h_2} I_2(l_2)\frac{\exp(-j\beta R_{y2})}{R_{y2}}dy_2'\right\} \tag{11}$$

A_{x1} and A_{y1} in (9) are related with A_{x2} and A_{y2} by (12).

$$\begin{bmatrix} A_{x1} \\ A_{y2} \\ A_{z3} \end{bmatrix} = \begin{bmatrix} \cos\theta & 0 & \sin\theta \\ 0 & 1 & 0 \\ -\sin\theta & 0 & \cos\theta \end{bmatrix}\begin{bmatrix} A_{x2} \\ A_{y2} \\ A_{z2} \end{bmatrix} \tag{12}$$

Once ABCD matrix is obtained by substituting (9) into (8), the voltage and the current at each terminal can be calculated.

4. Calculated and Measured Results

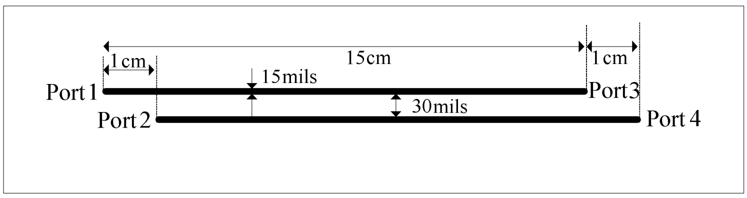

Figure 4: A schematic model of shifted parallel-coupled lines

The calculated crosstalk responses for the shifted parallel-coupled lines on a PCB like the structure in Fig. 4 are compared with the measured results and simulated ones using HFSS. The relative permittivity and the thickness of the dielectric material are ε_r=4.6 and t=47 mils, respectively. The width, the length of line, and the separation between coupled lines are 15 mils, 150 mm, and 30 mils, respectively. The calculated, measured, and simulated results of near-end crosstalk and far-end crosstalk for the structure in Fig. 4 are shown in Fig. 5.

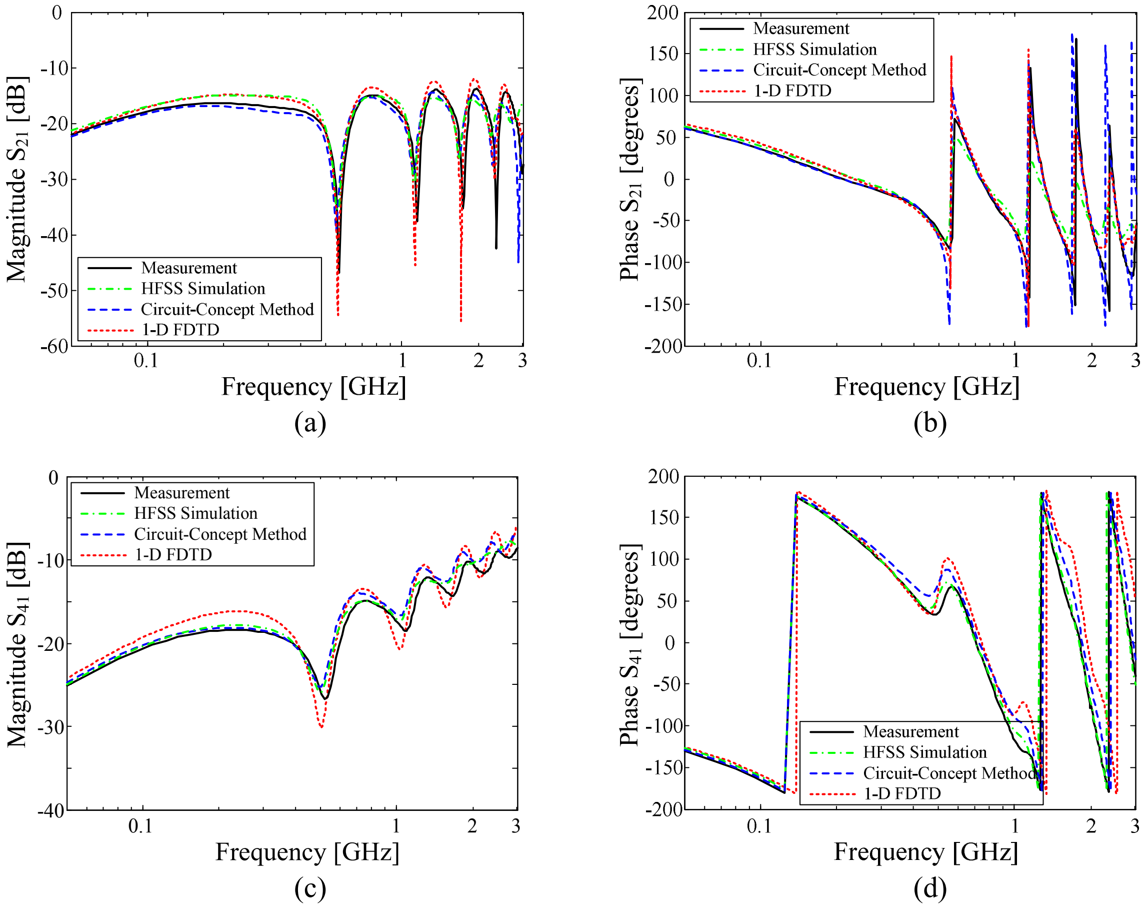

Figure 5: Near-end and far-end crosstalk characteristics of the model in Fig. 4, (a) Magnitude of S_{21}, (b) Phase of S_{21}, (c) Magnitude of S_{41}, (d) Phase of S_{41}

5. Conclusions

We have studied the crosstalk between shifted parallel-coupled lines on a PCB by using 1-D FDTD equations and circuit-concept approach. The calculated results by two theoretical approaches are compared with the measured ones and simulated ones using HFSS. The results are in good agreement. In the future, we will study the coupling phenomena between MTLs including via fence and bent line structure using 1-D FDTD method and compare the results with those of other approaches.

Acknowledgments

This research was supported by the MIC (Ministry of Information and Communication), Korea, under the ITRC (Information Technology Research Center) support program supervised by the IITA (Institute of Information Technology Advancement) (IITA-2006-(C1090-0603-0034)).

References

[1] C. R. Paul, *Analysis of Multiconductor Transmission Lines*, New York, Wiley-Intersciences, 1994.

[2] J. C. Ju, S. W. Park, J. H. Lee, and D. C. Park, “1-D FDTD equations for calculation of crosstalk on a PCB having a guard trace with vias,” *2004 Korea-Japan Joint Conference on AP/EMC/EMT*, Seoul, Korea, pp. 293-297, 2004.

[3] Y. Kami and W. Liu, “Analysis of coupling between transmission lines in arbitrary directions,” *IEEE Intn. EMC Symp.*, Denvor, CO, pp. 952-957, 1998.